



The 4th ICMSc
2022

Number : 2131/UN17.7/PP/2022

CERTIFICATE OF ACHIEVEMENT

The 4th International Conference on Mathematics and Sciences (ICMSc) 2022
proudly presents this certificate to

Igor Levi Satriani

as a

PRESENTER

in the conference that was held in Science Learning Center,
Faculty of Mathematics and Natural Sciences, Mulawarman University,
Samarinda - East Borneo, Indonesia. October 10th - 11th 2022.

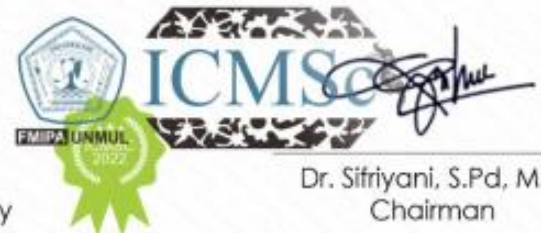
Theme :

"The roles of tropical science in new capital nation planning"

Faculty of Mathematics and Natural Sciences
Mulawarman University



Dr. Eng. Idris Mandang, M.Si
Dean FMIPA Mulawarman University



Dr. Sifriyani, S.Pd, M.Si
Chairman



FMIPA UNMUL

International Conference On Mathematics and Sciences

The 4th ICMSc
2022

**Optimalization of HIT
(*Heterostructure with
Intrinsic Layer*)
Solar Cell Efficiency with
Doping Layer**



Meet Our Team



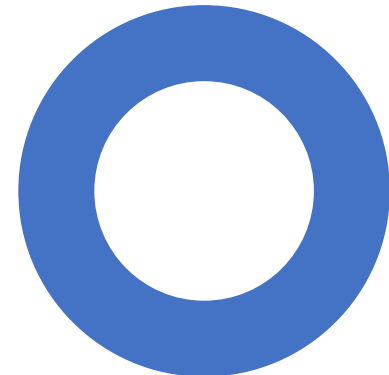
Dr. Dadan Hamdani, M.Si



Igor Levi Satriani

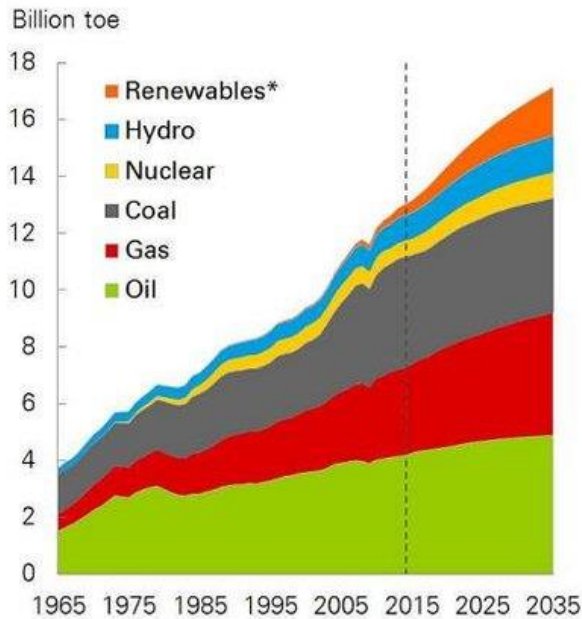


Rahmat Fadhillah

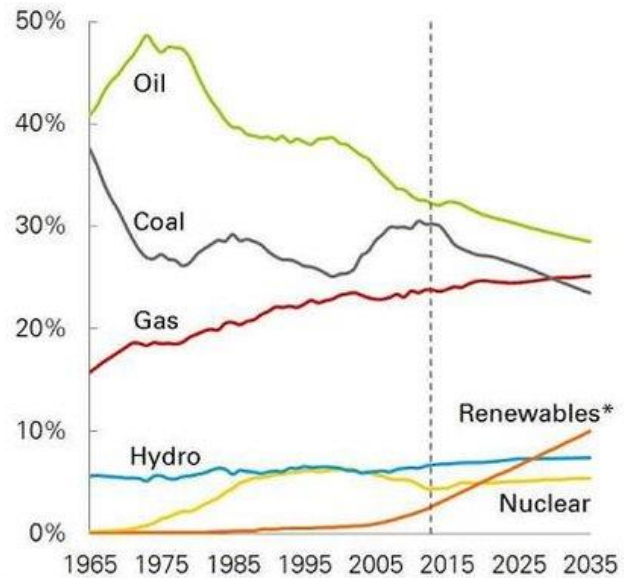


Energy Consumption

Primary energy consumption by fuel



Shares of primary energy



*Renewables includes wind, solar, geothermal, biomass, etc.

Arias, (2018).doi:10.3390/en11071617

GHG's Emission

Fossil fueled industries has become the largest GHG's emission. Its causing many major environment issues such as global warming or even an extreme climate changes.



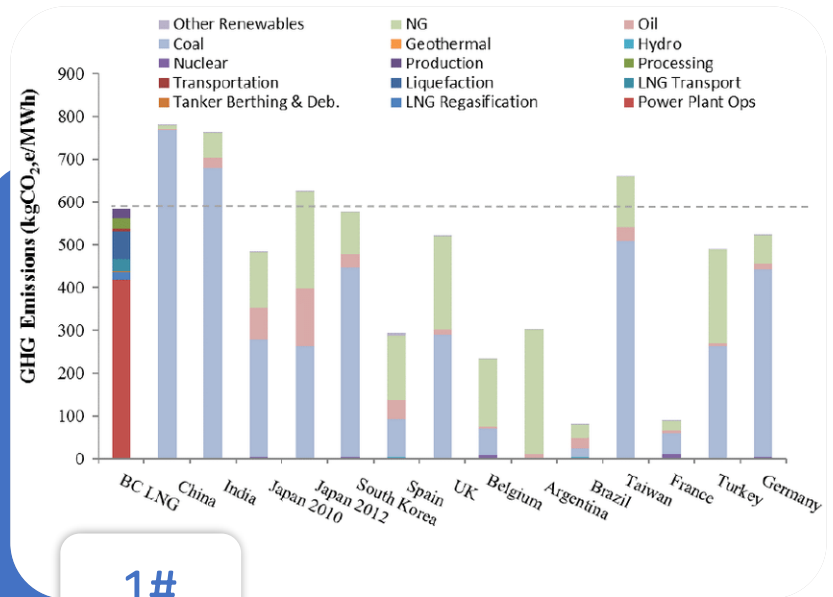
~80%

More than 80% of total emission produce by fossil fuel



700+ kgCO₂/MWh

China were the top country produces GHG's emission



1#
Coal Powered Industries


Coleman, J (2018), doi:10.1021/acs.est.7b05298

PV Tech generations

Three generations of PV technologies

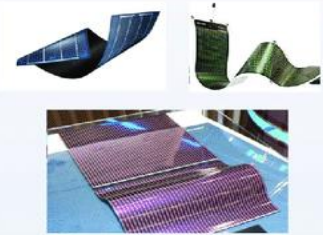
First generation solar PV cells

Single-crystal or monocrystalline silicon
 Polycrystalline or multicrystalline silicon



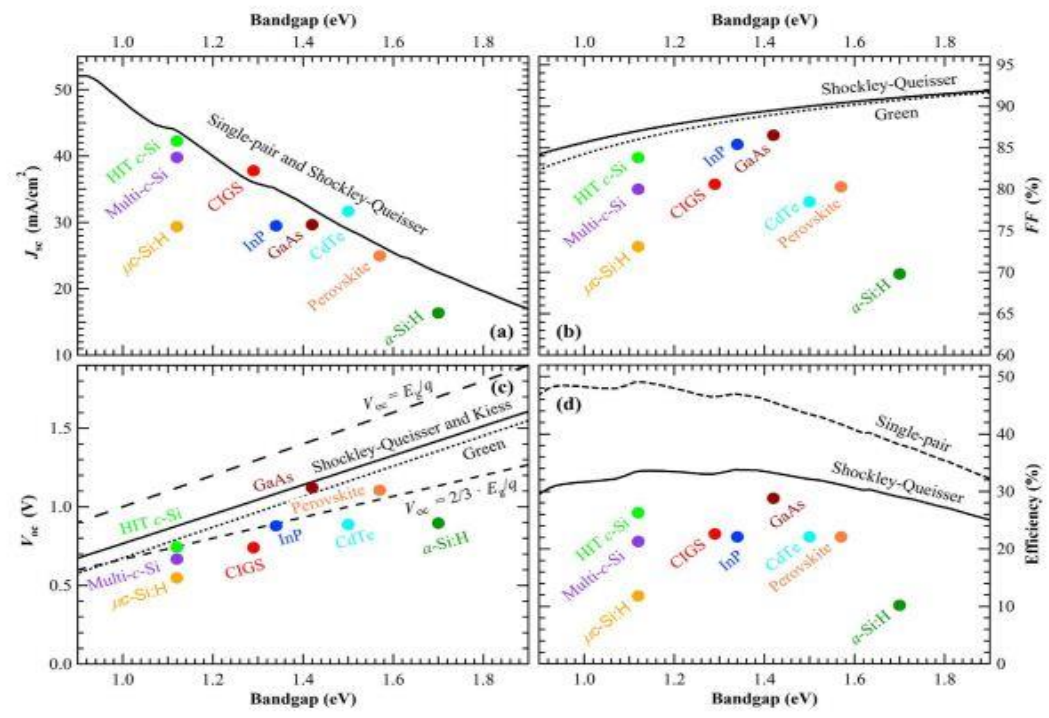
Second generation solar PV cells

Amorphous silicon (a-Si)
 cadmium telluride (CdTe),
 copper indium gallium selenide (CIGS)

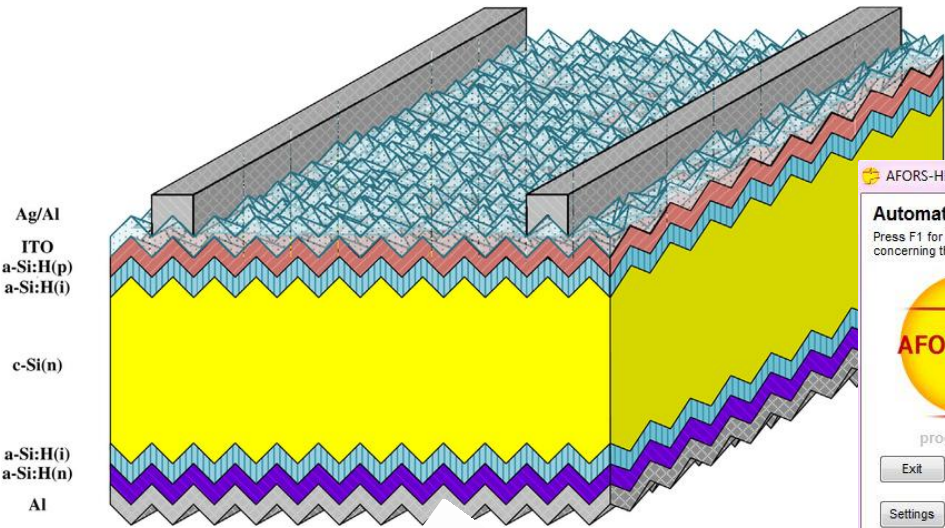


Third generation solar PV cells

Copper zinc tin sulphide (CZTS) PV cell
 Organic solar cell
 Perovskite Solar Cell
 Polymer PV cell
 Hybrid Solar Cell
 Buried Contact Solar Cell
 Concentrated PV Cell (CVP)
 Luminescent Solar Concentrator (LSC) Cell
 Multijunction Solar Cell (MJ)
 Nanocrystal Solar Cell
 Quantum Dot Solar Cell
 Dye-Sensitized Solar Cell (DSSC)
 Photoelectrochemical Cell (PEC)
 Etc.

HIT & AFORS-HET



AFORS-HET v2.5
Automat FOR Simulation of HETero structures
Press F1 for help concerning the active window.

external parameters

illumination
 On
 spectral
 monochromatic

Side
 Front
 Back

Measurement list
 I-V
 1DM
 I-V2DNet
 QE
 PEL
 TR-PEL
 intTR-PEL
 VD-SPV
 WD-SPV
 ID-SPV
 TR-SPV
 Goodman
 IMP
 ADM
 C-V
 C-T
 QSSPC
 PMCC
 EDMR
 show only latest graph

program control
Exit Define Structure
Settings Spectra Results

Parameter Variation
Set Go

Parameter Fit / Optimization
Set Go Results

Calculation
mode: Eq DC AC transient

Temperature
device temperature [K]: 300

Boundary
zero potential at positive pole

Boundary control DC:
 ext. Voltage [V]
 ext. Current [A/cm²]
0,000000000E+0
0,000000000E+0

Initial values for calculation:
Save Load
Initialize Calculate

Initialization Eq finished Problem Solved, iteration: 6, accuracy: 1,40122943893496E-16, GP/DGL 1/2

Main Goal

01

Validate HIT Solar Cell structure model by analysing 'Figure of Merits' (FOMs)

02

Enhancing HIT Solar Cell performance with simulation input parameters.

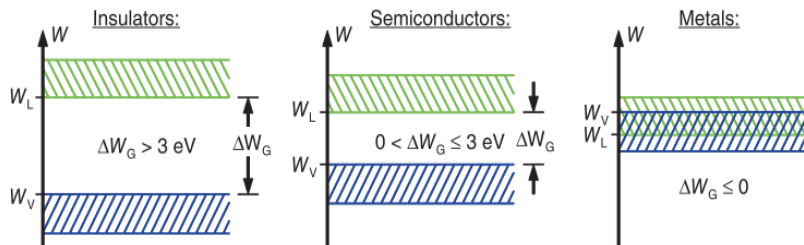
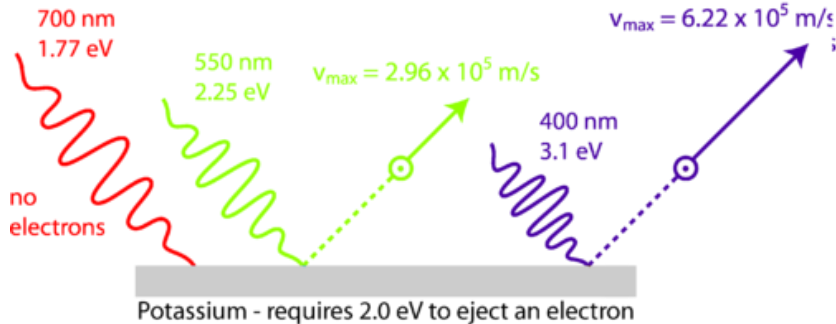
03

Getting the results of numerical data analysis for structure modelling that could be used on fabricated solar cell

Photovoltaic Introduction

Photoelectric effect

$$E_{\text{photon}} = h\nu$$

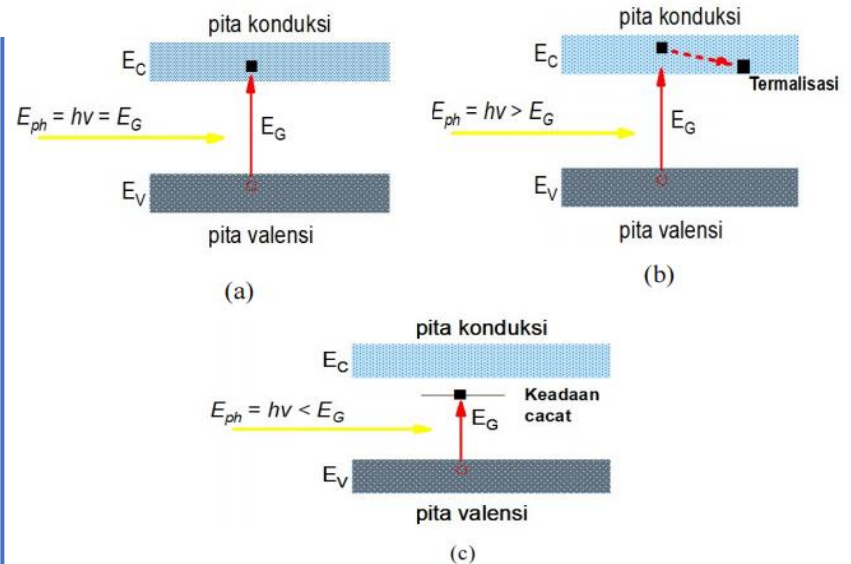


$$E^2 = (m_0 c^2)^2 + p^2 c^2$$

$$E^2 = p^2 c^2$$

$$E^2 = \left(\frac{h}{\lambda}\right)^2 c^2$$

$$E = \frac{hc}{\lambda} = h\nu$$



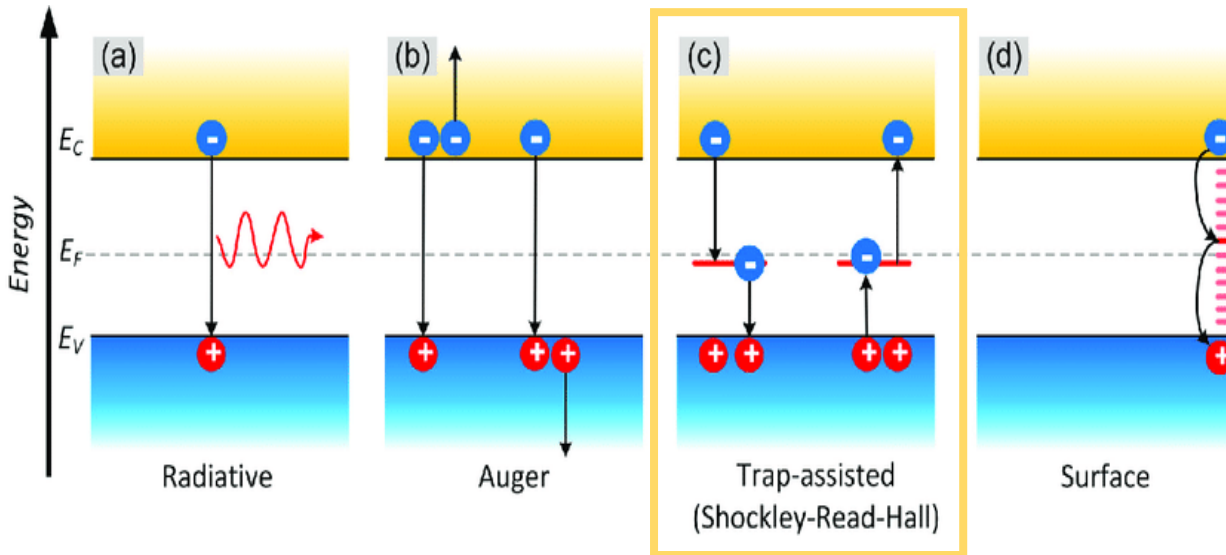
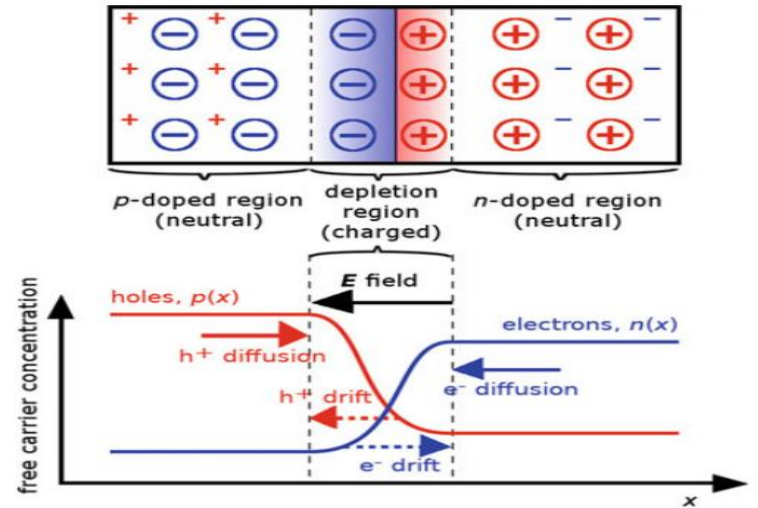
Material	Bandgap		References
	Value	Nature ^a	
Crystalline silicon (c-Si)	1.12	Indirect	[6, 7]
Hydrogenated microcrystalline silicon (μc-Si:H)	1.12	Indirect	[4]
Hydrogenated amorphous silicon (a-Si:H)	1.7-1.9	Non-direct	[4]
Crystalline germanium (c-Ge)	0.67	Indirect	[6, 7]
Hydrogenated amorphous germanium (a-Ge:H)	1.1	Non-direct	[4]
Hydrogenated amorphous Si-Ge alloys (a-Si,Ge:H)	1.1-1.8	Non-direct	[4]
Indium arsenide	0.36	Direct	[7]
Cadmium telluride (CdTe)	1.49	Direct	[6]
Copper indium selenide CuInSe ₂	1	Direct	[8]
Copper-indium-gallium-selenide (CIGS) (Cu _x In _y Ga _z Se ₂)	1-1.7	Direct	[8]
Kesterite {Cu ₂ ZnSn(S,Se) ₄ }	1-1.5	Direct	[8]
Cuprous oxide (Cu ₂ O)	2	Direct	[9]
Zinc telluride (ZnTe)	2.25	Direct	[6]
Gallium arsenide (GaAs)	1.43	Direct	[6]
Pyrite (FeS ₂)	0.95	Direct	[10]

^aSee Sect. 3.2.2 for the description of direct, indirect and non-direct bandgaps

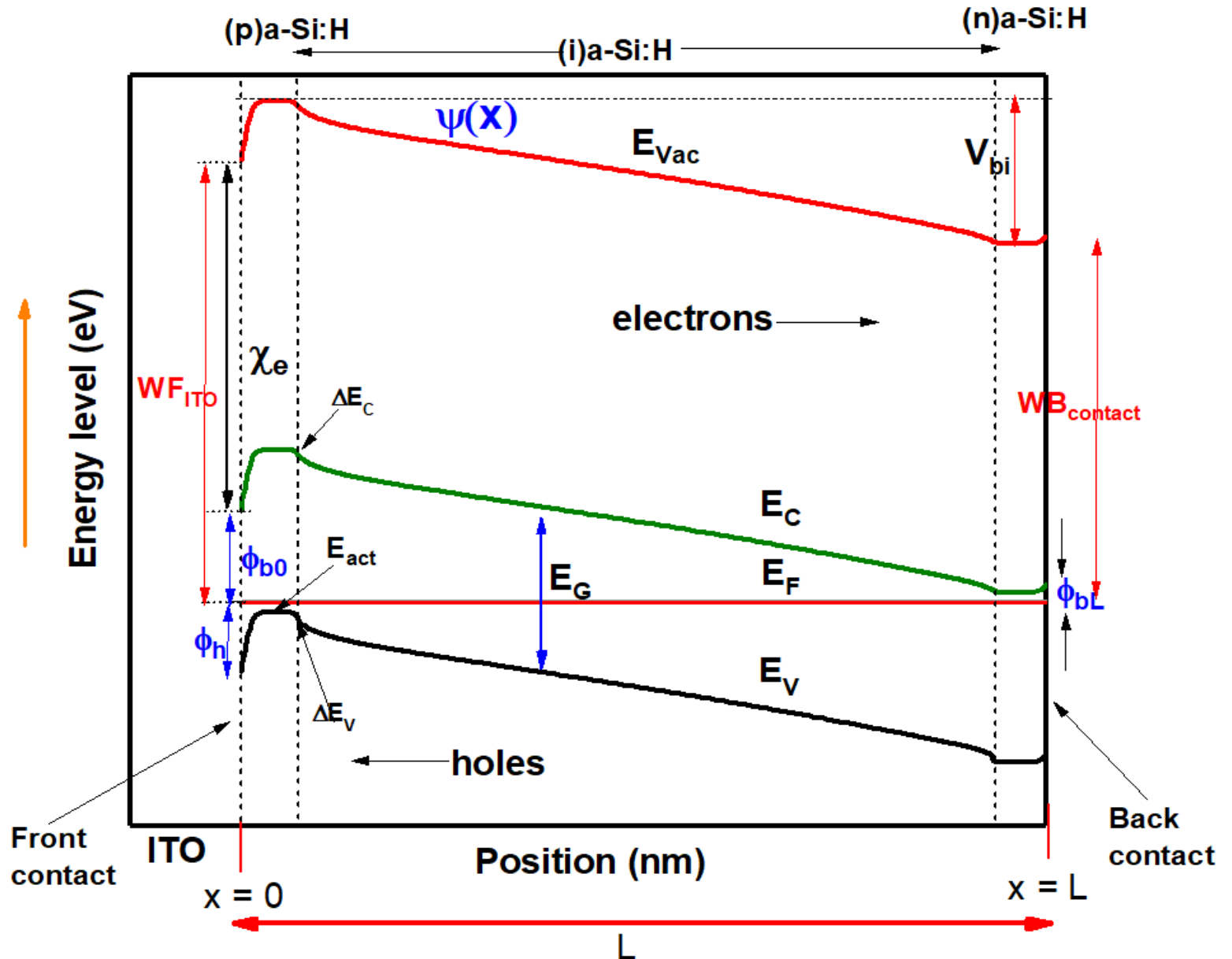
Recombination and Generation

SRH (Shockley-Read-Hall) Recombination, it emerge caused by defect on crystalline structures.

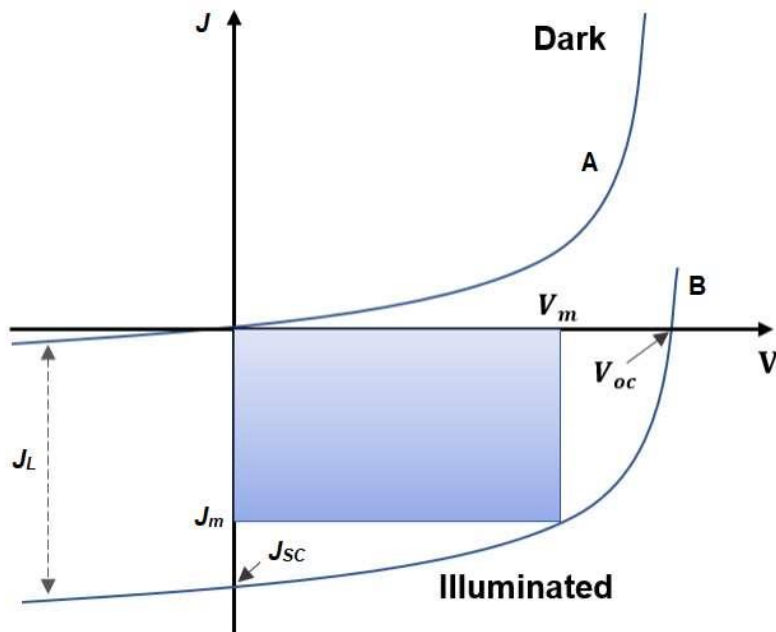
It involving E_{trap} appearing, causing electrons on conduction band also holes on valence band to recombine each other.



Energy Band Diagram



I-V Characteristics



Key Parameters

$$J_{sc} = 80 \text{ (mA/cm}^2\text{)} - 34 \left(\frac{\text{mA}}{\text{cm}^2\text{eV}} \right) \times E_G$$

$$V_{oc} = \frac{kT}{q} \ln \left(\frac{J_{ph}}{J_0} + 1 \right) \approx \frac{kT}{q} \ln \left(\frac{J_{ph}}{J_{00}} \right) + \frac{E_G}{q}$$

$$FF = \frac{V_m \times J_m}{V_{oc} \times J_{sc}}$$

$$E_{ff} = \frac{P_{maks}}{P_{input}} = \frac{FF V_{oc} J_{sc}}{P_{input}}$$

$$J_{dark} = J_0 \left(e^{\frac{qV}{kT}} - 1 \right)$$

$$J_0 = J_{00}^{green} \times e^{\left(\frac{-E_g}{kT} \right)} \quad ($$

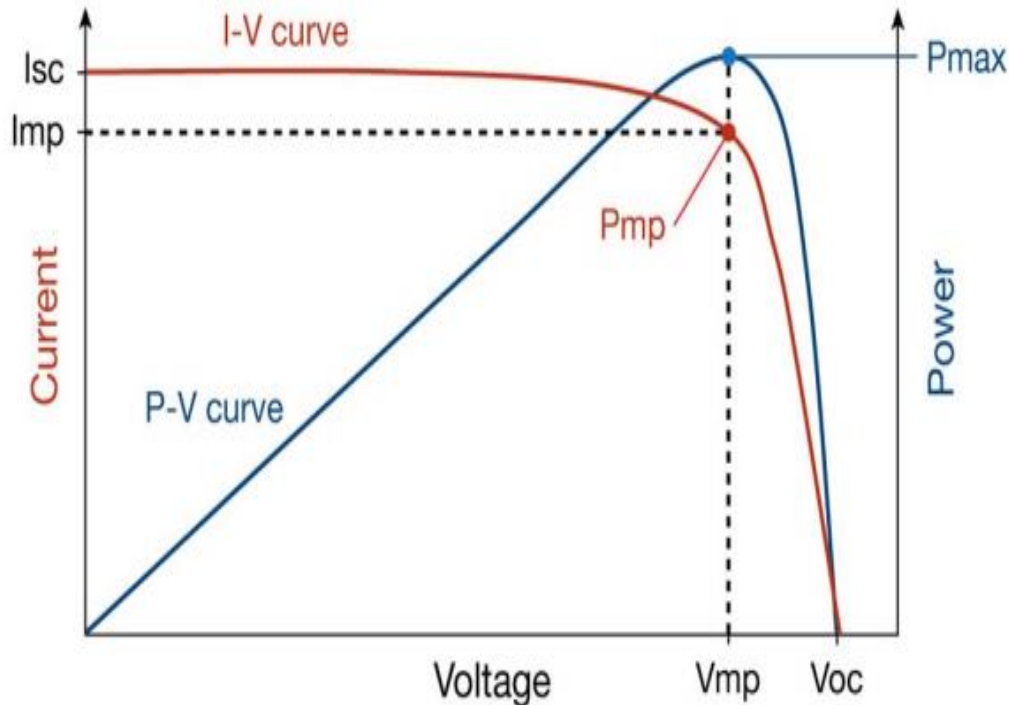
$$J_0 = 1,5 \times 10^8 \times e^{\left(\frac{-E_g}{kT} \right)} \quad ($$

With J_{00}^{green} as a factor green worth of 1×10^8 (Shah, 2020)

$$J_{illum} = J_{ph} - J_{dark}$$

$$J_{illum} = J_{ph} - J_0 \left(e^{\left(\frac{qV}{kT} \right)} - 1 \right)$$

FOMs (Figure of Merits)



Electrical Models

$$J_{sc} = 80 \text{ (mA/cm}^2\text{)} - 34 \left(\frac{\text{mA}}{\text{cm}^2\text{eV}} \right) \times E_G$$

$$V_{oc} = \frac{kT}{q} \ln \left(\frac{J_{ph}}{J_0} + 1 \right) \approx \frac{kT}{q} \ln \left(\frac{J_{ph}}{J_{00}} \right) + \frac{E_G}{q}$$

$$FF = \frac{V_m \times J_m}{V_{oc} \times J_{sc}}$$

$$E_{ff} = \frac{P_{maks}}{P_{input}} = \frac{FF V_{oc} J_{sc}}{P_{input}}$$

Optical Models

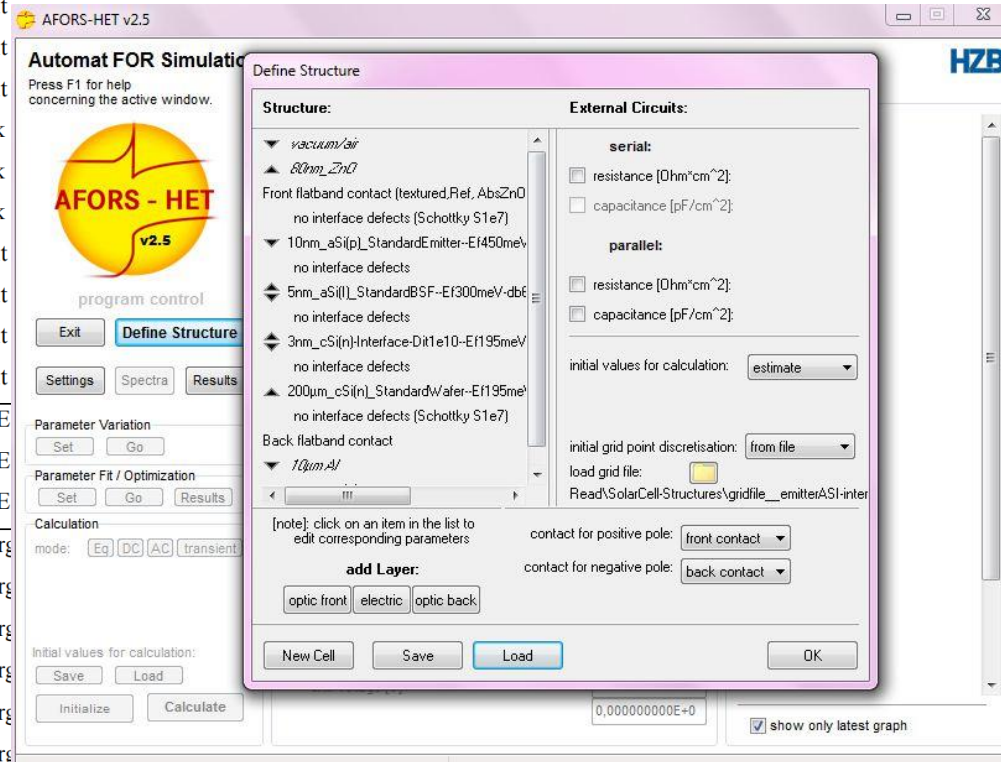
$$EQE = \frac{J_{sc} \left(\frac{hc}{\lambda} \right)}{q I_0(\lambda)}$$

Short circuit

$$IQE = \frac{EQE}{1-R}$$

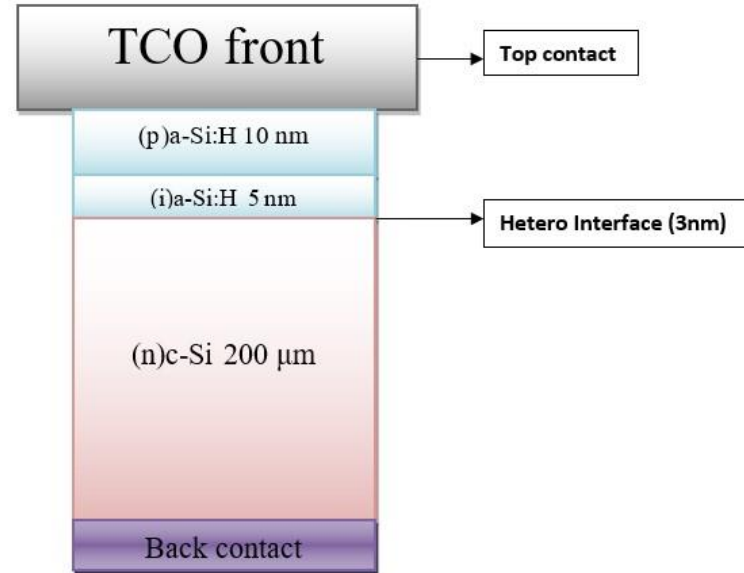
Charge Carrier

Parameter	Besaran	Satuan	Model Analisis
Electrical FOMs	J_{sc}	mA/cm ²	Kurva J-V Light
	V_{oc}	mV	Kurva J-V Light
	J_m	mA/cm ²	Kurva J-V Light
	V_m	mV	Kurva J-V Light
	J_0	mA/cm ²	Kurva J-V Dark
	$J_0, Schottky$	mA/cm ²	Kurva J-V Dark
	n	-	Kurva J-V Dark
	R_s	Ω.cm ²	Kurva J-V Light
	R_{shunt}	Ω.cm ²	Kurva J-V Light
	FF	%	Kurva J-V Light
E_{ff}	%	Kurva J-V Light	
Optical FOMs	EQE	%	Karakterisasi QE
	IQE	%	Karakterisasi QE
	SR	A/W	Karakterisasi QE
Analisis	Height barrier ϕ_{b0}	eV	Diagram pita energi
	Height barrier ϕ_{n0}	eV	Diagram pita energi
	Height barrier ϕ_{pL}	eV	Diagram pita energi
	Band offset konduksi ΔE_C	eV	Diagram pita energi
	Band offset valensi ΔE_V	eV	Diagram pita energi
	Surface band bending	eV	Diagram pita energi
	Medan listrik internal E_{int}	V/cm	Profil medan listrik
	Laju rekombinasi total	cm ⁻³	Profil laju rekombinasi
	Konsentrasi pembawa muatan	cm ⁻³	Profil pembawa muatan



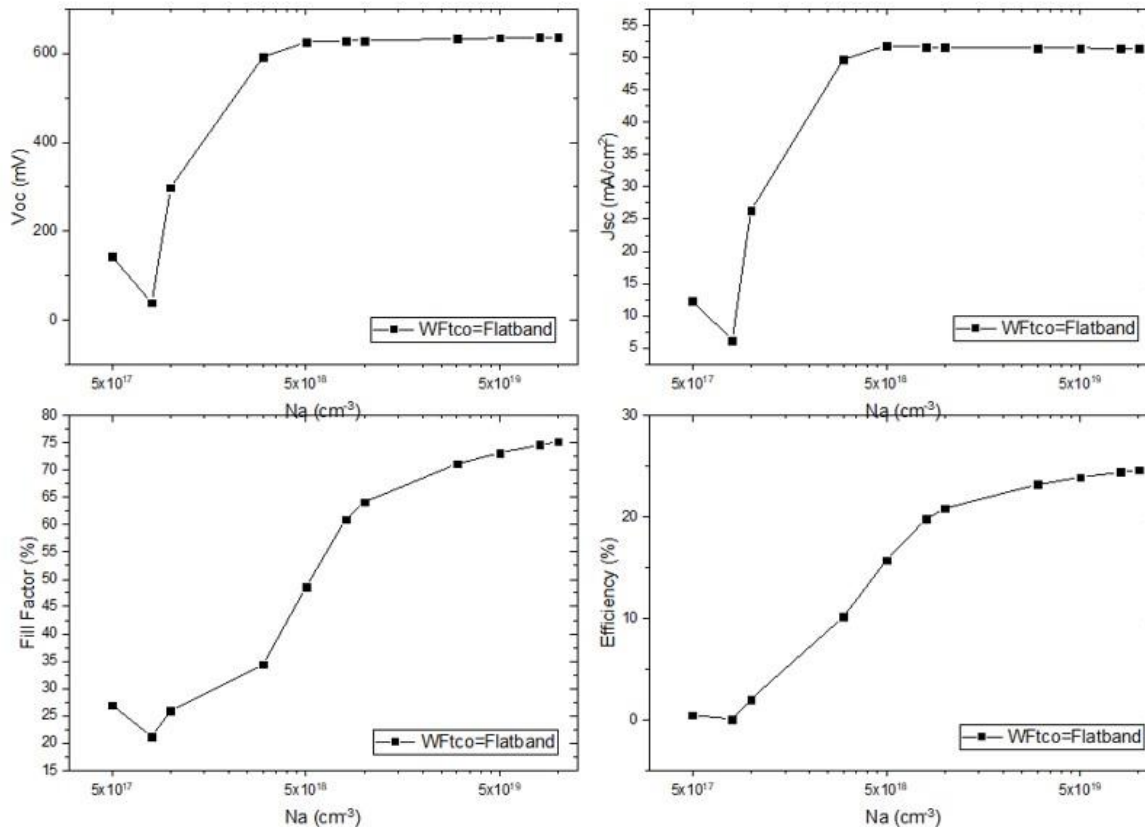
Input Parameters

Parameters	(p')a-Si:H	(i)a-Si:H	a-Si:/c-Si interface	(n)c-Si
Thickness (nm)	10	5	3	2×10^5
Dielectric constant	11.9	11.9	-	11.9
Electron affinity (eV)	3.9	3.9	-	4.05
Band gap (eV)	1.72	1.72	-	1.124
Effective conduction tape meeting (cm^{-3})	2.5×10^{20}	2.5×10^{20}	-	$2,846 \times 10^{19}$
Effective valence band meeting γ (cm^{-3})	2.5×10^{20} 1.0×10^{17}	2.5×10^{20}	-	$2,685 \times 10^{19}$
Acceptor concentration, N_a (cm^{-3})	5.0×10^{17} 1.0×10^{20}	0	-	0
Donor concentration, N_d (cm^{-3})	0	0	-	1.5×10^{16}
Electron mobility ($\text{cm}^2 \text{V}^{-1} \text{s}^{-1}$)	20	20	-	1111
Hole mobility ($\text{cm}^2 \text{V}^{-1} \text{s}^{-1}$)	5	5	-	421.6
Thermal rate for electrons ($\text{cm}^{-3} \text{s}^{-1}$)	1.0×10^7	1.0×10^7	-	1.0×10^7
Thermal rate for holes ($\text{cm}^{-3} \text{s}^{-1}$)	1.0×10^7	1.0×10^7	-	1.0×10^7
The tightness of the defects on the edges of the conduction band (valence) ($\text{cm}^{-3} \text{eV}^{-1}$)	4.0×10^{21} (4.0×10^{21})	2.0×10^{21} (2.0×10^{21})	-	1.0×10^{14} (1.0×10^{14})
Urbach energy for the tail of the conduction band (valence) (eV)	0.06(0.03)	0.094(0.068)	-	-
Capture cross section σ_c (σ) conduction (cm^2)	1.0×10^{-17} (1.0×10^{-15})	7.0×10^{-16} (7.0×10^{-16})	-	-
Capture cross section σ_c (σ) for the tail of the valence band (cm^2)	1.0×10^{-15} (1.0×10^{-17})	7.0×10^{-16} (7.0×10^{-16})	-	-



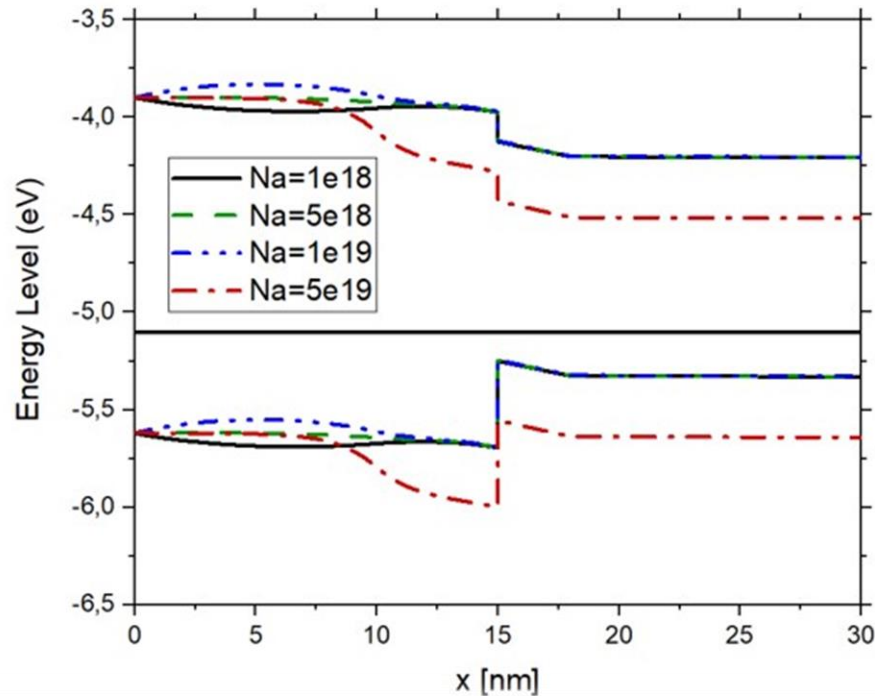
Gaussian state meeting (cm^{-3})	1.0×10^{18} - 1.5×10^{19}	7.0×10^{19}	-	-
Gaussian peak energy for donors (acceptors) (eV)	1.22(0.70)	0.5(0.60)	-	-
Gaussian standard deviation for donors (acceptors) (eV)	0.23(0.23)	0.21(0.21)	-	-
Capture cross section σ_c (σ) for donor-like Gaussian states (cm^2)	1.0×10^{-14} (1.0×10^{-15})	3.0×10^{-14} (3.0×10^{-15})	-	-
Capture cross section σ_c (σ) for acceptor-like Gaussian states (cm^2)	1.0×10^{-15} (1.0×10^{-14})	3.0×10^{-15} (3.0×10^{-14})	-	-
Total DOS D_n (cm^{-2})	-	-	1.0×10^9 1.0×10^{11}	-
Midgap density of satay ($\text{cm}^{-3} \text{eV}^{-1}$)	-	-	-	1.0×10^{10}
Characteristic energy (eV)	-	-	-	0.56
Capture cross section for donor-like (cm^2)	-	-	1.0×10^{-14} (1.0×10^{-14})	1.0×10^{-14} (1.0×10^{-14})
Capture cross section for acceptor-like (cm^2)	-	-	1.0×10^{-14} (1.0×10^{-14})	1.0×10^{-14} (1.0×10^{-14})

Doping Optimization



Using various doping at 5×10^{17} cm⁻³ up to 1×10^{20} cm⁻³ observed. Doping with $N_a = 5 \times 10^{18}$ cm⁻³ shows a rapid improvement on Voc & Jsc, with 15.73% Solar cell Efficiency

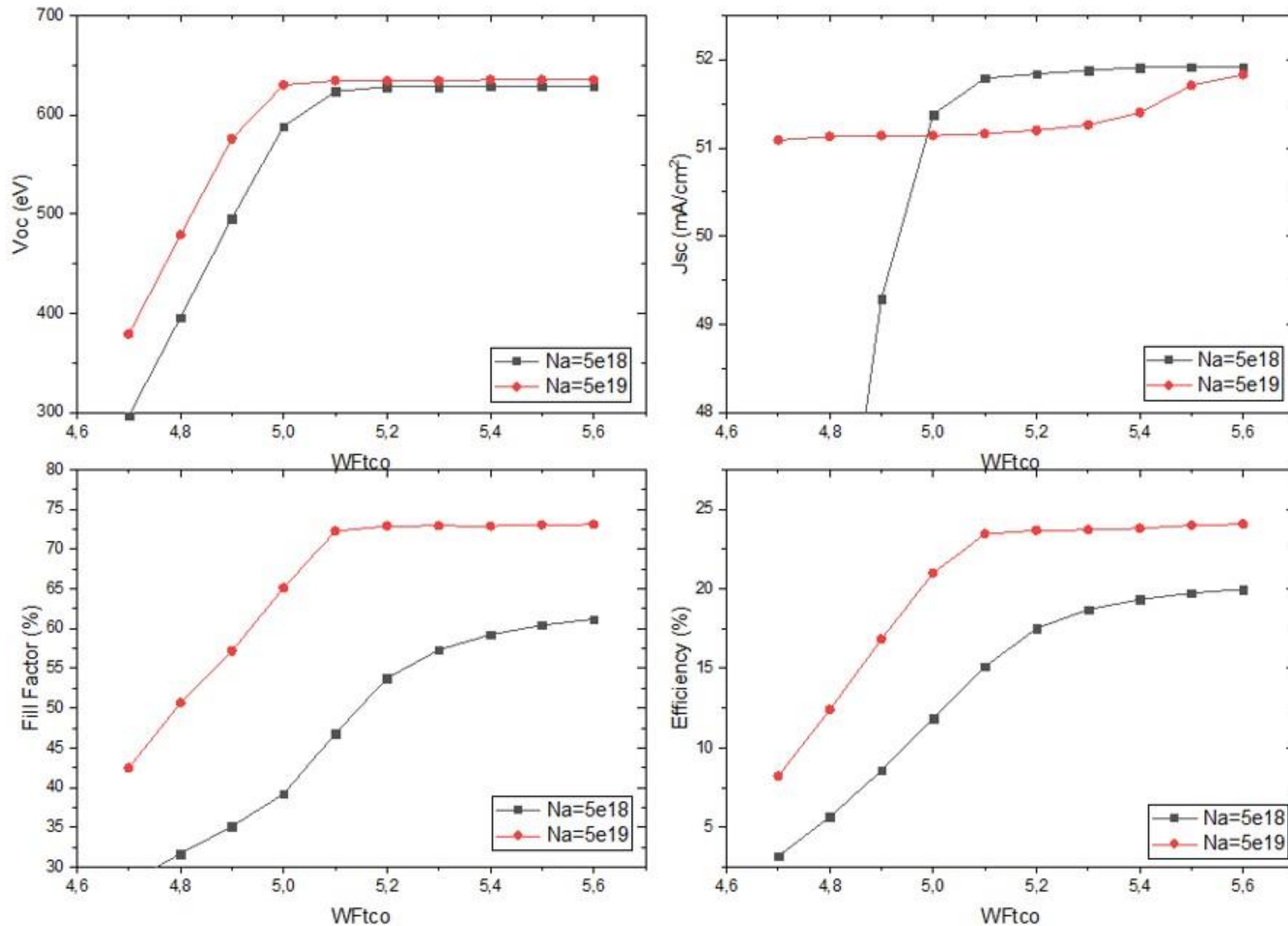
Doping Optimization



Band Diagram with various doping N_A

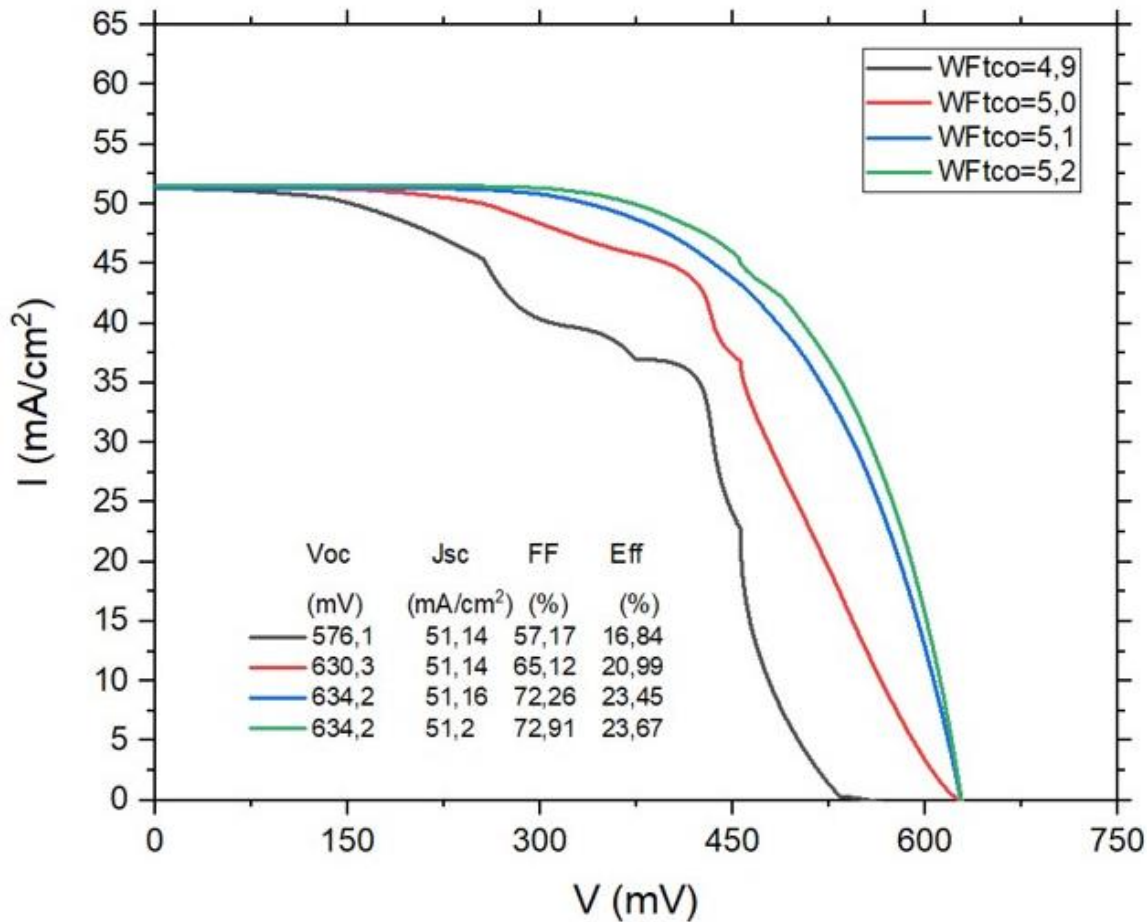
With increasing doping N_a given on (p+) layer. Valence Energy band to move away from fermi level energy, need a higher energy for electron to excite.

WFtco Optimization



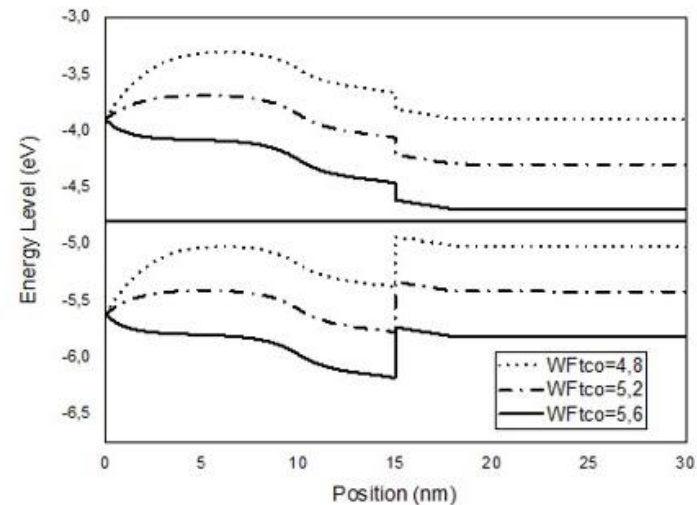
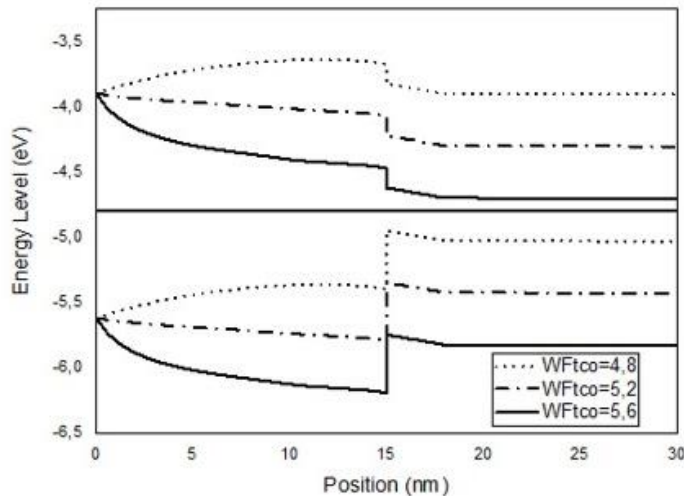
Using optimum doping N_a , to achieve an effective Wftco Value for improving solar cell performance

WFtco Optimization



characteristic curve on HIT solar cells with TCO/(p+/i)a-Si structure:H/(n)c-Si/Al with variations in WF_{tco} values with AM1.5G irradiation spectrum and stable temperatures at 300K. Then also used the doping concentration of N_A at optimum concentrations, namely $5 \times 10^{19} \text{ cm}^{-3}$

WFtco Optimization

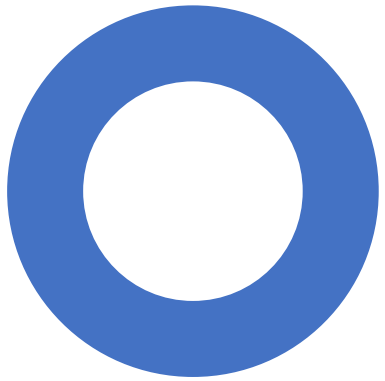


$$\varphi_B = (\chi_{a-Si:H} - E_{G(a-Si:H)}) - WF_{tco}$$

- At the value of WFtco < 5.0 eV, a significant decrease in the Voc voltage and the formation of Jsc current was found. Causes decreased performance of solar cells. The initial assumption is due to the formation of potential-barriers in the interface of the front-facing layer with the layer (p+) so that Schottky contact arises in this area of the interface
- At the WF tco value ≥ 5.0 eV, it experienced a significant increase in the Voc voltage and Jsc current when compared to the lower WFtco value. However, with the increasing value of the work function of the front contact, it is not monitored for significant changes with the Voc value ranging at 4 mV and Jsc in the range of 0.06 mA/cm².

Summary

- The provision of optimum NA acceptor doping concentration with variations from minimum to maximum doping shows that the N_a doping value significantly improves performance at $5 \times 10^{18} \text{ cm}^{-3}$ and keeping stable at $5 \times 10^{19} \text{ cm}^{-3}$. So that from the results of the WFtco variation, the value of the front contact work function used was optimal and combined with the N_a doping input so that the optimum result was shown at the doping condition $NA = 5 \times 10^{19} \text{ cm}^{-3}$ and the optimal WFtco at WFtco = 5.2 eV where the FOMs parameter value ($V_{oc} = 634.2 \text{ mV}$) was obtained; $J_{sc} = 51.2 \text{ mA/cm}^2$; $FF = 72.91 \%$) obtained optimum solar cell performance efficiency of 23.67%
- In the use of varied WFtco values, it was found that the occurrence of Schottky barrier on the front contact interface of the TCO/(p+)a-Si:H for a relatively smaller WFtco value ($< 5.0 \text{ eV}$), resulted in trapping the hole so that it could not move towards the front contact. Then at a high WFtco value ($> 5.0 \text{ eV}$) there is a tendency to form Ohmic contacts where a reverse barrier is formed so that hole injection into the (p+)a-Si:H layer and band-bending is increasingly visible, allowing the hole to be able to move to the front contact.



Thank You

